A Speed-based Model for Crowd Simulation Considering Walking Preferences

Sainan Zhang[1], Jun Zhang[1], Mohcine Chraibi[2], and Weiguo Song[1]

[1]State Key Laboratory of Fire Science, University of Science and Technology of China, Hefei, 230027, China

[2]Institute for Advanced Simulation. Forschungszentrum Jülich GmbH, Jülich, 52428, Germany

Corresponding author: Jun Zhang (e-mail: junz@ustc.edu.cn).

Abstract To investigate the influence of the walking preferences on pedestrian movements, a modified collision-free speed model is proposed by considering the expectations of comfortable walking for a pedestrian. In the model, the walking directions of pedestrians are determined by taking human perception of comfort and preference for walking straight to their intended destinations into account. The restriction of walls in heading direction on pedestrian's walking is introduced to avoid potential collisions among pedestrians and obstacles. Model validation with respect to experimental data shows that our model performs better than the original model with regards to the trajectory's distribution and the velocity profile, and can effectively alleviate backward movements. Furthermore, the speed-density relation in corridor inferred from the new model fits the experimental data well and the model performs more accurately in simulating the flow-width relation in bottleneck scenario than the original collision-free speed model.

Keywords: Collision-free speed model, pedestrian dynamics, walking preference

1. Introduction

Dense crowds formed due to holidays or large scale activities are often related to risks, such as stampede[1,2]. To improve the safety of events, a variety of pedestrian models have been proposed to uncover the mechanism of individual behaviors and interactions among pedestrians and obstacles[3–7].

In the force-based models[8], the evolution of pedestrian movement over time is described by the Newtonian dynamics. Several self-organized phenomena like arching at bottlenecks and lane-formation in bidirectional flow[9,10] can be reproduced fairly well. However, pedestrians in these models are regarded as moving particles under the influence

of forces, which often leads to unrealistic backward movement and overlapping when the repulsive forces from neighbors and obstacles are larger than the self-driven force, especially under high densities[11]. Moreover, forces in these models are often defined to be long-ranged, which means that invisible or even pedestrians in a large distance still influence the movement of their neighbors. A usually used remedy is to introduce an artificial cut-off radius. In addition, force-based models require solving second-order differential equations with a small time step, which causes a high computational overhead[12].

Another category of models is velocity-based[13–16]. Here pedestrian's speed is adjusted based on the relative positions and velocities of their neighbors. Compared to force-based models, they deal with overlapping among pedestrians efficiently with a reduced computational cost. However, these models often depend on a large number of parameters, which causes inherent calibration difficulties. The collision-free speed model[12] realizes collision avoidance solely depending on the minimum headway distance. Despite of its simplicity, it can reproduce many self-organization phenomena with higher efficiency.

In fact, besides the exclusion among people or obstacles, pedestrians are affected by many other factors when deciding the moving directions like their perception of comfort and preference for walking straight to the intended destinations[17–19]. However, models mentioned above do not take these differences into account. The heuristic model was proposed to predict the walking direction and displacement of pedestrians based on behavioral heuristics[20,21]. It makes a trade-off between seeking an unobstructed walking direction and minimizing detours from the most direct route. Nevertheless, it does not consider the critical acceptable distance for pedestrians to maintain the desired direction. For example, if there are other people or obstacles in its desired direction, no matter how far away, the pedestrian in this model will immediately react by changing the moving direction to avoid obstacles, which is not in line with reality. In the collision avoidance experiment in[22], the probability of pedestrian changing movement direction decreases exponentially as the headway distance increases when the distance is larger than 1.099 m.

Furthermore, the displacement is solved by two integration steps of the acceleration, which results in an increased computational expense.

To overcome these shortcomings, we developed a new microscopic model by integrating walking preferences of pedestrians into the collision-free speed model. Walking preferences include pedestrians' inclination for a desired direction, demand for a longer walking way than the least comfortable headway distance and tendency to following others' moving behaviors. Whereas from a modelling perspective, it is rather difficult to consider all these factors. In this paper, we only focus on the first two walking preferences, as we think they have a significant effect on pedestrian's movement.

The remainder of this article is structured as follows. The model is defined in section 2 while the validation and comparison between simulation results of collision-free speed model and proposed model are shown in section 3. In section 4, we discuss parameter's influence on the results and the limitation of the model. Finally, we give a summary of the model in section 5.

2. Model definition

As for the walking preferences, pedestrians' inclination for desired direction and demand for a longer walking way other than the least comfortable headway distance are considered. The proposed model is composed of two parts: a direction submodule and a speed submodule. Within this approach, the actual moving direction is obtained based on two walking preferences. First, a pedestrian has a strong expectation to maintain its desired direction unless the obstacle in the moving direction makes the walking uncomfortable[23]. Second, in case the direction of motion has to be changed, it is desirable to maintain the deviation from the desired direction as small as possible[24]. Finally, the influence of walls on the pedestrian's walking speed is introduced into the collision-free velocity model to achieve collision avoidance for pedestrians.

2.1. The direction submodel

The movement of a pedestrian can be affected by the neighbors nearby. Pedestrians in the front have stronger impact on one's movement than those in the rear and the closed

pedestrians have greater influence than those far away. Based on this assumption, only the pedestrians in the desired direction of the movement are regarded as neighbors in the model to maximize the computational efficiency of the model[12]. Here, we define the desired moving direction from the current pedestrian position to the final target point.

Accordingly, the neighbors of pedestrian *i* are defined as follows:

$$J_i = \{j, \vec{e}_{id} \cdot \vec{e}_{i,j} < 0 \text{ and } \left|\vec{e}_{id}^{\perp} \cdot \vec{e}_{i,j}\right| < l/s_{i,j}\}, \quad (1)$$

where j denotes other pedestrians (except pedestrian i), $\vec{e}_{id}$ represents the desired direction of pedestrian i, $\vec{e}_{id}^{\perp}$ is a vector obtained by rotating $\vec{e}_{id}$ for 90º counterclockwise, $\vec{e}_{i,j}$ is a unit vector from j to i, l denotes the diameter of pedestrians simplified to circles with same size, $s_{i,j}$ represents the Euclidean distance between the centers of pedestrians i and j. As shown in Fig. 1, neighbors of pedestrian i are those who overlap with the grey area.

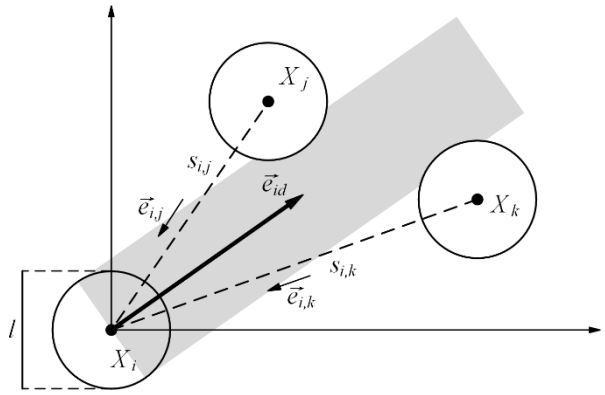

Fig. 1: A sketch showing the neighbors of pedestrian i. In this model, X_i, X_j and X_k are positions of pedestrians. $s_{i,j}$ and $s_{i,k}$ are distances between the centers of pedestrians. $\vec{e}_{i,j}$ and $\vec{e}_{i,k}$ are unit vectors from X_j and X_k to X_i.

The closest pedestrian $j_{\min}$ in the desired direction of motion is defined such that

$$s_{i,j_{\min}} = \min_{j \neq i} s_{i,j}. \quad (2)$$

As observed in people's daily behavior in shared places, people prefer to make a detour from their desired directions, when the comfortable walking space is occupied by others.

Considering pedestrian's preference for comfort during walking, we define the following condition:

$$s_{i,j_{\min}} < s_c. \tag{3}$$

As shown in Eq. (3), s_c represents the critical comfortable walking distance in different scenarios. That is, if the distance $s_{i,j_{\min}}$ for pedestrian i is smaller than s_c, the pedestrian will feel uncomfortable and prefer to pass the one ahead. Whether to take transcendental action or not, it ultimately depends on the size of the free space around. If a pedestrian decides to detour, deflecting minimally from the desired direction will be adopted.

When the condition (3) is met, pedestrian i will deviate from its desired direction and the change is minimized as far as possible. In this sense, two tangent directions $\vec{e}_{io}$ and $\vec{e}_{is}$ shown in Fig. 2 are considered as the best alternative choices. The corresponding deflection angle $\Delta\theta_o$ and $\Delta\theta_s$ can be calculated as:

$$\begin{aligned} \Delta\theta_o &= \left(\arcsin\frac{l}{s_i} - \arccos\left(\vec{e}_{id}\cdot\vec{e}_{ji}\right)\right)\cdot g\left(\vec{e}_{id}^{\perp}\cdot\vec{e}_{ij}\right) \\ \Delta\theta_s &= -\left(\arcsin\frac{l}{s_i} + \arccos\left(\vec{e}_{id}\cdot\vec{e}_{ji}\right)\right)\cdot g\left(\vec{e}_{id}^{\perp}\cdot\vec{e}_{ij}\right), \end{aligned} \tag{4}$$

where subscripts o and s are short for "optimal" and "sub-optimal", respectively. $\Delta\theta_o$ and $\Delta\theta_s$ represent the deflection angles required to turn from the desired direction $\vec{e}_{id}$ to $\vec{e}_{io}$ and $\vec{e}_{is}$. s_i denotes the distance from the center of pedestrian i to that of the nearest neighbor. Function $g(x)$ is 1 if $x > 0$, and otherwise is equal to -1. It is noted that when the conditions of optimal and suboptimal directions are the same, that is, $\vec{e}_{id}^{\perp}\cdot\vec{e}_{ij}$ is equal to 0, $g\left(\vec{e}_{id}^{\perp}\cdot\vec{e}_{ij}\right)$ will be -1, resulting in a negative value of $\Delta\theta_o$. Considering that y-axis is defined along the direction of the exit, x-axis is defined in accordance with the right-hand rule and the desired movement direction of pedestrian corresponds to the angle away from the x-axis, it can be found that the negative deflection angle $\Delta\theta_o$ makes the pedestrian choose the right side of the desired direction, which corresponds to the right-side preference of pedestrian for overtaking[25].

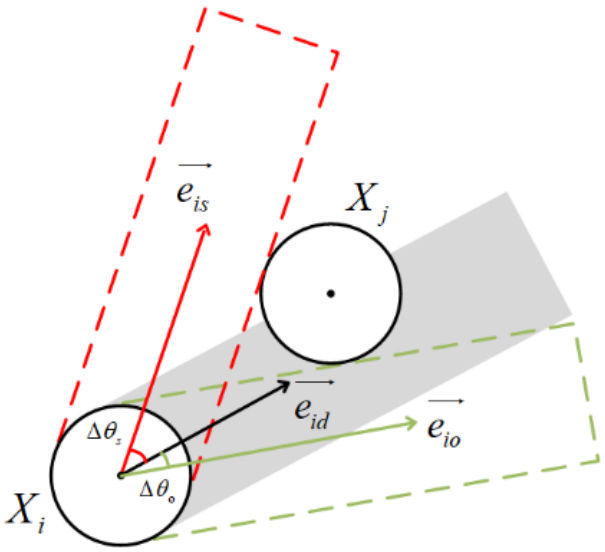

Fig. 2: A sketch showing two tangent directions $\vec{e}_{io}$ and $\vec{e}_{is}$. $\vec{e}_{io}$ represents the direction with minimum deflection angle to surpass the pedestrian ahead. $\vec{e}_{is}$ represents the direction with minimum deflection angle in the opposite deflection of $\vec{e}_{io}$.

Based on this idea, we calculate the final deflection angle as defined in Eq. (5). Where k_o and k_s represent the pedestrian's choices of $\vec{e}_{io}$ and $\vec{e}_{is}$. Only two values 0 and 1 can be chosen.

$$\Delta\theta = k_o \cdot \Delta\theta_o + (1 - k_o) \cdot k_s \cdot \Delta\theta_s. \tag{5}$$

The value of k_o and k_s is determined by the minimum acceptable distance and actual free space in the new direction. Specifically,

$$\begin{cases} k_o = s_r^o(i,j,t) > s_{im} \text{ and } s_r^o(i,w,t) > s_{im} \\ k_s = s_r^s(i,j,t) > s_{im} \text{ and } s_r^s(i,w,t) > s_{im} \end{cases} \tag{6}$$

Here, j and w indicate the pedestrian and wall, respectively. $s_r^o(i,j,t)$ and $s_r^o(i,w,t)$ are parameters in $\vec{e}_{io}$ direction. Specifically, $s_r^o(i,j,t)$ and $s_r^o(i,w,t)$ represent the space from the nearest pedestrian and the movable distance from the nearest wall for pedestrian i when there are other pedestrians or walls in its direction. Similarly, $s_r^s(i,j,t)$ and $s_r^s(i,w,t)$) are parameters in the $\vec{e}_{is}$ direction. $s_r^s(i,j,t)$ and $s_r^s(i,w,t)$) represent the free space from the nearest pedestrian and the nearest wall in $\vec{e}_{is}$ direction. s_{im} denotes the minimum acceptable distance for pedestrian i.

Next, we illustrate how a pedestrian makes a detour. Based on the preference for the desired direction, a pedestrian considers the direction with smallest deviation firstly. That corresponds to $\vec{e}_{io}$ direction in Fig. 3. Then, the actual distance is compared with the minimum acceptable distance to decide which direction to choose. Only when both conditions $s_r^o(i,j,t) > s_{im}$ and $s_r^o(i,w,t) > s_{im}$ are satisfied, the pedestrian detours to $\vec{e}_{io}$ direction with the angle $\Delta\theta_o$. Otherwise, the other direction $\vec{e}_{is}$ is considered using the same criterion. When both conditions $s_r^s(i,j,t) > s_{im}$ and $s_r^s(i,w,t)) > s_{im}$ are met, it will choose the $\vec{e}_{is}$ direction with the angle $\Delta\theta_s$. If the conditions in both directions do not hold, the original movement direction will be kept without deflection.

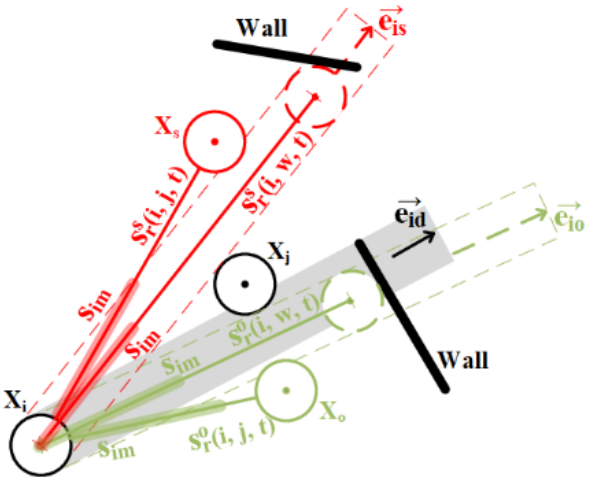

Fig. 3: A sketch showing elements in $\vec{e}_{io}$ and $\vec{e}_{is}$ directions. Red and green indicate the elements in $\vec{e}_{is}$ direction and $\vec{e}_{io}$ direction, respectively. The dashed circle represents the furthest position that the pedestrian can reach when there is a wall in the new direction.

The corresponding flow chart of direction model is shown in Fig. 4.

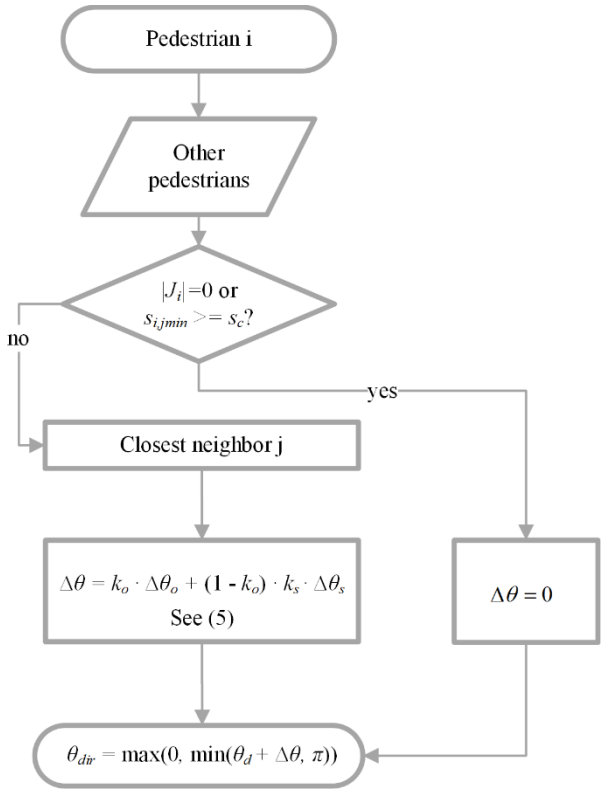

Fig. 4:The flow chart of the direction model. θ_{dir} represents the angle between actual movement direction and x-axis. We define that x-axis is the direction perpendicular to the exit direction. θ_d represents the angle between desired direction and x-axis.

2.2. The speed submodel

As defined in the collision-free speed model, the speed of pedestrian i is given by

$$v_p = \min\{v_0, \max\{0, (s - l)/T\}\}. \quad (7)$$

Where, v_0 is the free speed. T represents the time gap for a pedestrian to accelerate from static to v_0. s denotes the distance from the center of a pedestrian to that of its nearest neighbour.

However, in addition to other pedestrians, there are still some other obstacles and walls affecting the pedestrian's movement state and the magnitude of speed in real environments.

Based on these considerations, we introduce the effect of the wall into the original collision-free speed model. As shown in Fig. 5, s_{iw} represents the maximum distance a pedestrian can move when the movement direction is occupied by the wall. To realize no collisions with walls, a constraint of speed is added as follows:

$$v_w = \min\{v_0, s_{iw}/T\}. \tag{8}$$

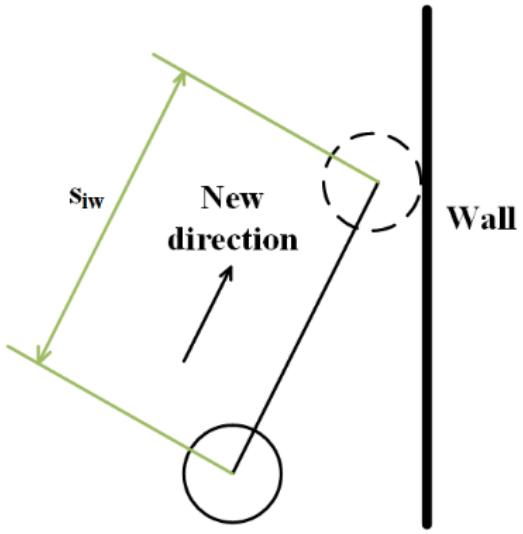

Fig. 5: The maximum distance that a pedestrian can move when the front is a wall. The solid circle represents the current position of the pedestrian. The dashed circle represents the furthest position that the pedestrian can reach when there is a wall in the new direction. s_{iw} represents the maximum distance a pedestrian can move with a wall in a new direction.

Combining the above constraints, the final speed model is defined as

$$v_p = \min\{v_0, \max\{0, (s-l)/T\}, s_{iw}/T\}. \tag{9}$$

3. Simulation results

In this section, we set up a series of simulations to verify and validate the model by comparing it with the original collision-free speed model and empirical findings. Several scenarios are considered, including narrow corridor, corridor with periodic boundaries and bottleneck. The simulations are executed with JuPedSim[26] using a time step $\Delta t = 0.04s$.

3.1. Test in narrow corridor

Firstly, we perform simulations in a narrow corridor as shown in Fig. 6. In this scenario, a pedestrian is set to move straight along the corridor, while another pedestrian is standing on the way. The free speed v_0 of the pedestrian is set as 1.6 m/s. T is equal to 1.0 s in both collision-free speed model (CFM) and the proposed model. The minimum acceptable distance s_{im} is equal to 0.1 m in $\vec{e}_{io}$ and $\vec{e}_{is}$ direction. s_c is the distance at current speed in a time step.

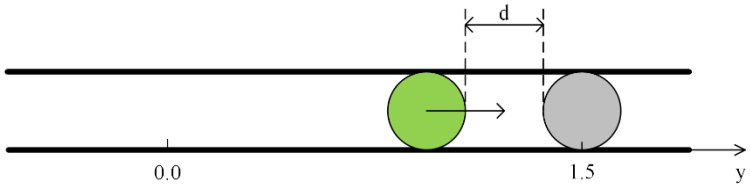

Fig. 6: A sketch of the test in narrow corridor. The corridor is very narrow such that only one person can pass at the same time. The green circle denotes the pedestrian who wants to go straight and the grey one indicates the person standing in the corridor.

The positions of the pedestrian during the movement in both models are shown in Fig. 7. It is clear that the moving pedestrian in the CFM starts to oscillate in a certain distance to the pedestrian in front. The occurrence of such oscillations is due to the superpositive nature of its destination sub-model. However, the pedestrian stays close to the static one without oscillations in our model.

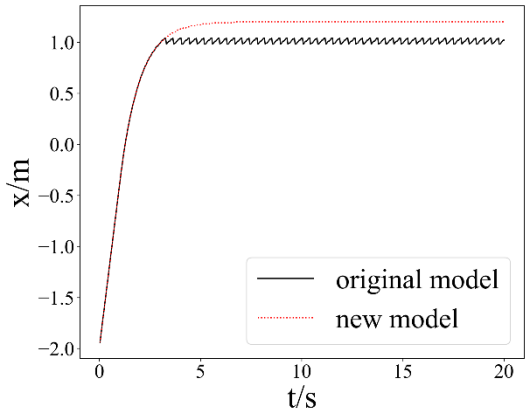

Fig. 7: The position of the moving pedestrian versus time. While the original model shows an erroneous oscillatory behavior, the trajectory simulated by our proposed model is smooth and shows no oscillations.

3.2. Corridor with periodic boundaries

To further verify and validate the model, we carry out a simulation in a $30 \times 1.8\ m^2$ corridor with periodic boundary conditions and compare the results with the experimental data downloaded from the website[1].

Fig. 8 shows the sketch of the experiment scenario, which is composed of two $6\ m$ long straight corridors and two semicircular corridors with the inner radius $2.0\ m$. The width of the corridor is $1.8\ m$. Pedestrians were distributed uniformly along the oval corridor at the beginning of the experiment and then they were asked to walk clockwise at a normal speed. In the experiment, different crowd densities were formed by changing the number of the participants in the corridor.

[1] http://doi.org/10.34735/ped.2009.13

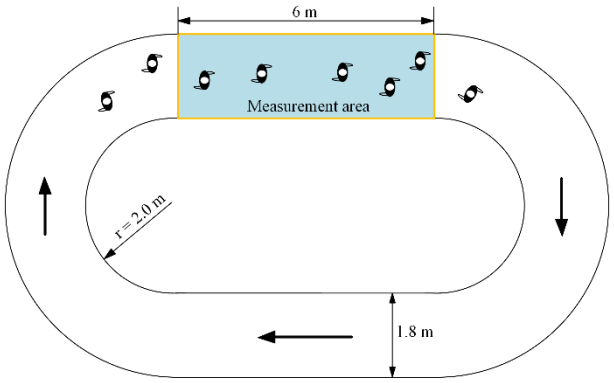

Fig. 8: The sketch of the experiment scenario. The measurement area is set in the straight corridor with the length of 6 m and width of 1.8 m.The pedestrians were asked to move in the direction shown by the arrow in the oval corridor.

Considering that the desired directions of pedestrians in this scenario are parallel to each other and there are little competition among them for side-wise movement space, we make the critical distance of the detour s_c consistent with the distance of 0.1 times free velocity in speed model. The parameter setup of the new model is shown in table 1. The shape of pedestrian is circular with a constant diameter l, which is determined by the highest density in the experiment. Specifically, we calculate the average area occupied by each pedestrian in the high-density area in the experiment. Then the diameter of the equivalent circle under the same area is calculated as the pedestrian size. Based on the experiment data, we get the value of l 0.36 m. T is the ratio of pedestrian interval to the moving speed defined in Eq. (9) before the one reaches the free velocity. Pedestrian intervals and speed under different densities in the experiment are calculated and then we get the value of T 0.86 s. The parameters of the original model(CFM) are from[27] and shown in table 2. The strength coefficient k is 3.0. The distance coefficient D is 0.1 m. The experimental data with 15 participants (the minimum number of participants) are selected to obtain the free speed of pedestrians with the consideration that the average interval is 2 m, which is enough for pedestrians to walk at the free speed when the participants are distributed uniformly in the corridor. Based on this, we get the mean value of the free speed 1.186 m/s and a standard deviation of 0.05 m/s.

Table 1: Parameters of pedestrian and model in corridor with periodic boundary scenario. where, $s(x)$ denotes the minimum distance when the speed is x, which is consistent with Eq. (9).

l	s_c	s_{im}	T
0.36	$s(0.1v_0)$	$s(v_0)$	0.86

Table 2: Parameters of pedestrian and CFM in corridor with periodic boundary scenario.

l	k	D	T
0.36	3.0	0.1	0.86

We use method D in[28] to calculate the density and speed of pedestrians in the measurement area. As shown in Fig. 9, with the increase of the crowd density, the movement speed of the crowd decreases. It is worth noting that when the crowd density is greater than 3 m^{-2}, the speed decreases very slowly and is mostly less than 0.2 m/s. These results of CFM and new model both fit well with the experiment.

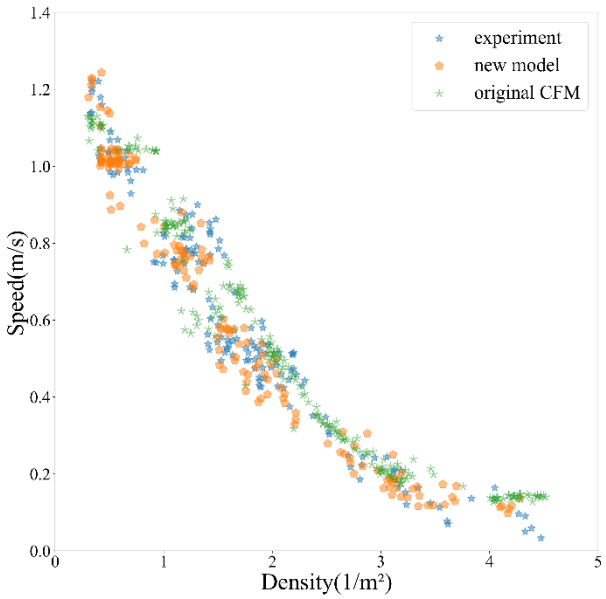

Fig. 9: The relationship between speed and density. Blue, orange and green represent the results of experiment, new model and original CFM, respectively.

3.3 Bottleneck

In order to test the rationality of the model in the bottleneck scenario, we set up the model's simulation scenario referring to the setting in the experiment[29].

The parameters of the new proposed model are shown in table 3. v_t is the moving speed of pedestrian in current frame. The free speed of pedestrians are obtained from the experiment scenario with the bottleneck of length 0 m where the pedestrians move relatively freely after walking out of the bottleneck. The free speed follows a normal distribution with a mean value of 1.200 m/s and a standard deviation of 0.249 m/s. The time gap T is obtained based on the ratio of pedestrian interval to walking speed in the experiment. The value of T is 0.61 s. Considering the desired directions of pedestrians in this scenario are intersecting so that the competition among them for movement space is more intense than that in corridor scenario, we make the critical distance of the detour s_c consistent with the distance of free velocity in speed model. The strength coefficient k and the distance coefficient D in CFM are shown in table 2.

Table 3: Parameters of pedestrian and new model in bottleneck scenario.

l	s_c	s_{im}	T
0.36	$s(v_0)$	$s(v_t)$	0.61

Trajectories and spatial profiles of velocity and density of pedestrians are shown in Fig. 10[29]. We can intuitively find that the trajectories follow a cone distribution in the experiment due to the normal walking without pushing in the experiment. Compared with the trajectories distribution from the CFM, which is like an arching shape, the trajectories obtained from our model are more similar to those of the experiment. Moreover, comparing the velocity profiles among the experiment, CFM and new model, we find some common characteristics of them. Firstly, the velocity of pedestrians in front of the bottleneck entrance is relatively uniform. This may because the pedestrians are congested before the narrowing in both models, while in the experiment, according to the recorded video,

pedestrians rarely take surpass behavior and they enter the bottleneck with an orderly manner, which leads to the similar moving state of pedestrians. Secondly, pedestrians in the bottleneck are in an accelerated state, which may due to the increase of the exit attraction as the pedestrian approaches the exit. Furthermore, although the bottleneck limits the moving space, the speed in it is higher than in front of it, which is due to the lower density and competition in the bottleneck. Compared with the velocity profile from the CFM, the speed calculated by the new model describes the velocity profile of the experiment better. From the density profiles, it is found that the density in the bottleneck decreases as the distance to exit decreases, since the pedestrians ahead are in an accelerated moving state so that the distance between the agents becomes larger and the density becomes lower. In addition, although the densities in front of the bottleneck entrance obtained from the new model are higher than that of the experiment, a visible enhancement can be observed compared with the density profile from the CFM.

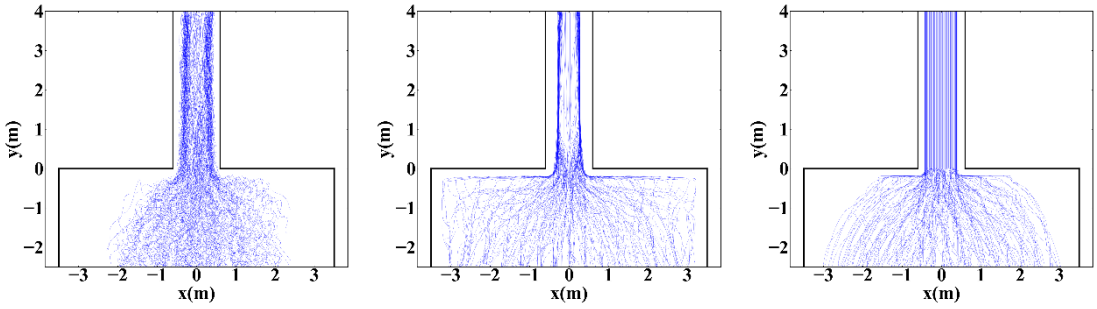

(a) Trajectory, experiment (b) Trajectory, CFM (c) Trajectory, new model

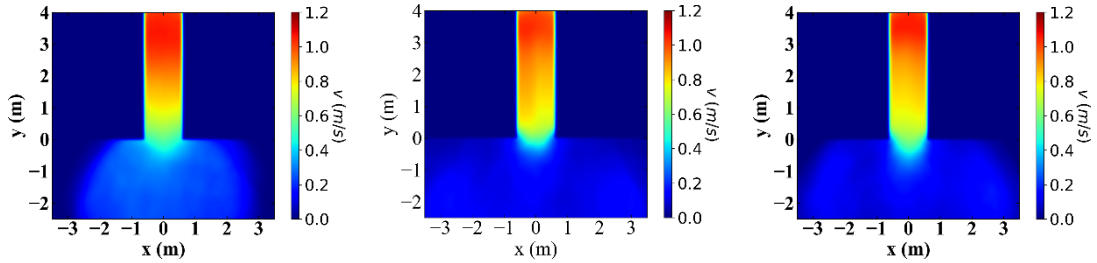

(d) Velocity, experiment (e) Velocity, CFM (f) Velocity, new model

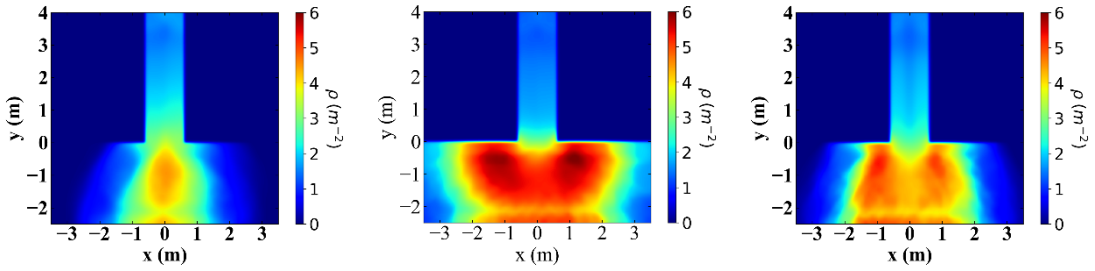

(g) Density, experiment (h) Density, CFM (i) Density, new model

Fig. 10: Trajectories and spatial profiles of velocity and density in the experiment and simulations. Pedestrians passed through the bottleneck from the bottom to top. The width of the bottleneck is 1.2 m. Columns from left to right show the data from experiment, CFM and new model, respectively. Rows show the trajectories, velocity profile and density profile from top to bottom, respectively.

To validate the model quantitatively, we further analyze the relationship between the flow and bottleneck width by adjusting the bottleneck width from 1.0 m to 2.5 m in our simulation. Here, we choose the line at the middle of the bottleneck as measurement line to calculate the flow defined in Eq. (10). For each bottleneck width, ten runs are performed and the mean of these results is shown in Table 4.

$$flow = (N-1)/\Delta t. \tag{10}$$

Where, N is the number of participants in the experiment. Δt represents the time interval between the first and the last person passing the measurement line.

Table 4: Pedestrian flow in bottleneck scenario.

$Width/m$	$Flow/(s^{-1})$			$Relative\ error(e)/\%$	
	Exp	CFM	New	$e(CFM)$	$e(New)$
1.0	1.791	1.302(±0.024)	1.701(±0.046)	27.33	5.02
1.1	1.952	1.568(±0.029)	1.885(±0.049)	19.68	3.43
1.2	2.258	1.735(±0.036)	2.079(±0.044)	23.15	7.91
1.4	2.644	1.954(±0.030)	2.407(±0.084)	26.11	8.98
1.6	2.688	2.386(±0.054)	2.767(±0.126)	11.24	2.95

1.8	3.397	2.677(±0.052)	3.102(±0.066)	21.21	8.69
2.0	3.375	3.009(±0.045)	3.434(±0.096)	10.84	1.73
2.2	3.783	3.313(±0.072)	3.784(±0.168)	12.43	0.03
2.5	4.797	3.712(±0.078)	4.301(±0.083)	22.61	10.35
mean error/%	/	/	/	19.40	5.45

Values between brackets represent the standard deviation of pedestrian flow.

The relative error is calculated as

$$\frac{|experiment\ flow - simulation\ flow|}{experiment\ flow} \times 100\%$$

As can be seen from Table 4 and Fig. 11, with the increasing bottleneck width, the pedestrian flow increases in the experiment and both models. Further comparing the relative errors between the results of the two models and that of the experiment, it can be found that the relative errors from the new model are smaller than those obtained from the CFM.

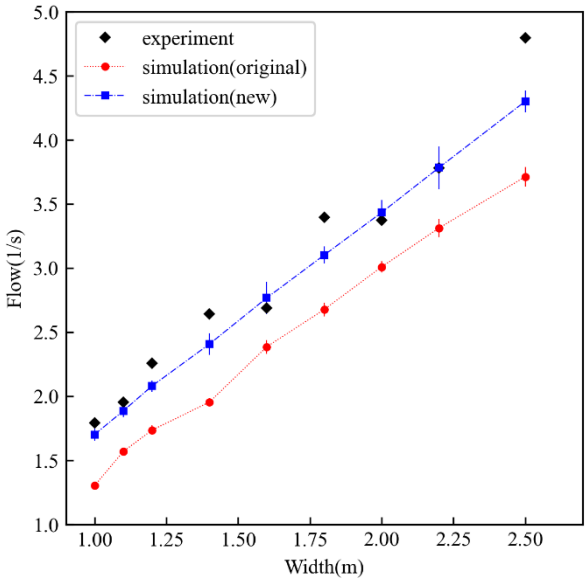

Fig. 11: The relationship between flow and bottleneck width. Rhombus, circle and square represent the results of experiment, CFM and new model, respectively.

Next, to test whether our model can effectively alleviate the backward movement of pedestrians in the bottleneck scenario, we calculate the angle between the actual movement

direction and the y-axis (We assume that the y-axis direction is consistent with the direction along the exit) during the entire movement in bottleneck scenario. When the angle is larger than $\pi/2$, we regard it as a backward movement. The results of angles are shown in Fig. 12. As we can observe, there is a part of pedestrians moving backwards in the original model, whereas this backward movement is strongly reduced in the new model which is more consistent with the experimental data. Therefore, the new model alleviates unrealistic backward movement effectively.

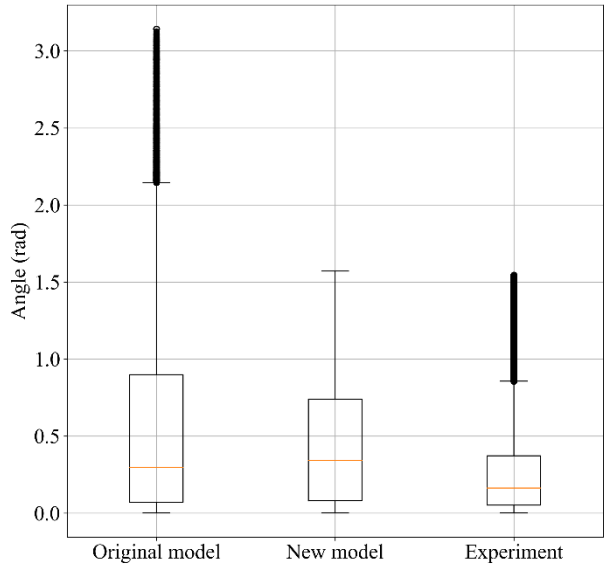

Fig. 12: The angle between pedestrian's moving direction and y-axis during the entire movement in bottleneck scenario. The box plots on the left, middle and right are from the CFM, new model and experimental data, respectively.

4. Discussion

The parameters and the limitation of the model are discussed in this section. The values of parameters depend on the situation and they may change in different scenarios. The possible reasons are as follows: in straight corridors with periodic boundary conditions, all pedestrians are expected to move straight. Hence, their desired movement directions are parallel so that there is little competitive behavior during walking. In this case, pedestrian's motion inertia dominates the movement and the intention to turn is not strong. However, in the bottleneck scenario, this behavior changes, since the bottleneck limits the movement space of pedestrian. In the simulation, the desired directions of

362 pedestrians point to the bottleneck entrance. As the crowd gets closer to the bottleneck, the
363 desired directions of pedestrians tend to intersect, so that the competition between
364 pedestrians is intensified. This may lead to a decrease in pedestrians' inertia influence,
365 resulting in more frequent steering maneuvers. In order to increase the probability of
366 obtaining free space as soon as possible, pedestrians will force themselves to react faster,
367 which leads to the decrease of T. s_c denotes the critical comfortable distance for pedestrian
368 to maintain the desired direction. When there is more competitive behavior during walking,
369 pedestrians will prefer larger value of s_c to make them feel comfortable. Factors affecting
370 s_{im} are similar to that of s_c. That is, the more intense the competition, the smaller the
371 minimum acceptable distances in the new direction. Therefore in straight corridor with
372 periodic boundary, s_{im} and T conditions are larger than in the bottleneck scenario, whereas
373 s_c is the opposite.

374 While the trajectories and profiles of velocity and density of pedestrians obtained from
375 the new model are qualitatively more consistent with the experimental results than those
376 from the CFM, the distribution of pedestrian and the density before the narrowing obtained
377 from the new model are still divergent to the experiment to some extent. The shape of
378 trajectories in front of the bottleneck entrance from the experiment is more conical. The
379 density obtained from the new model is higher than the experimental results. The possible
380 reasons are as follows: first, the patience and humility of human are not considered in the
381 model, pedestrians are competitive at the entrance of the bottleneck, which results in more
382 pedestrians staying close to each other and waiting at the bottleneck entrance, while under
383 the non-emergency conditions in real life, pedestrians showcase a polite behavior, so they
384 pass through the bottleneck in an orderly manner, hence the density of crowd in front of
385 the bottleneck is lower. It is also confirmed in the experiment video that pedestrians enter
386 the bottleneck continuously, without excessive clustering or long waiting time before the
387 narrowing. Second, to make pedestrians in our model pass through the bottleneck, we use
388 strategy 2 in JuPedSim to set target for every pedestrian. The target setting which affects
389 the position of high-density area in the CFM and new model is shown in Fig. 13. In the
390 model, the room is divided into three areas. Pedestrians in area 1 and area 3 try to move
391 towards target 1 and target 2, respectively. Pedestrians in area 2 are expected to walk

straight. Compared with the density profiles shown in Fig. 10, it is found that pedestrians in both two models cluster around the target point and lead to high density of nearby areas. In both two models, the target point for each pedestrian is static and never be changed in front of the bottleneck entrance. However, the target point for every pedestrian in real life may be dynamic and related to the surrounding environment, that is conductive to make people walk with less competition. At last, to improve the calculation efficiency, the pedestrians in the model are simplified to circles with equal diameters, which is different from the shape of people in daily life. When a pedestrian is in a stationary state, the shape of the real pedestrian is closer to an ellipse, which may also affect the form of the entire crowd distribution.

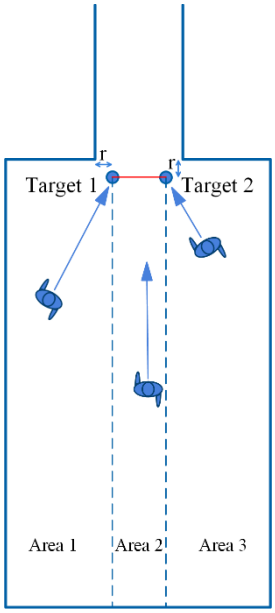

Fig. 13: A sketch shows the target setting in the CFM and the new model. Pedestrians in both two models aim to move based on the shortest distance to their target line.

The simulation results show that the model can simulate the pedestrians in bottleneck or corridor with periodic boundaries accurately, but it is not suitable for the counter-flow scenario. In reality, pedestrian's preferences in counter-flow are different from those in bottleneck or corridor with periodic boundaries. In the counter-flow scenario, before the formation of the layer, the potential conflict for pedestrians is greater than that in the other two scenarios. In this case, pedestrians are more inclined to avoid people further but moving in the opposite direction to avoid conflict, rather than overtaking the neighbor near

but in the same direction ahead. That is, even if the distance factor is not taken into account, pedestrians do not treat their neighbors equally. However, to simply the model, neighbors are treated equally by the pedestrian except for the distance factor. To improve the calculation efficiency, only the nearest neighbor is considered to determine the walking direction of pedestrian, no matter what the moving direction of neighbor is, which causes the congestion in counter-flow scenario. It's the limitation of this model which needs to be improved in the future. Validation of the model is geometry dependent. This is a clear limitation of the model's application and usability in complex evacuation scenarios. However, for understanding of phenomena emerging from pedestrian's movement in simple geometries, for example, the bottlenecks, our developed model is able to offer new insights and can be used as a valuable tool.

5. Conclusion

In this paper, we propose a microscopic pedestrian model by combining the pedestrian's walking preferences and collision-free speed model. We define the direction submodel by considering subjective factors of crowd, like perception of comfort and preference for walking straight to destination. The effect of walls is introduced in collision-free speed model to calculate the speed of pedestrians in normal motion. Finally, we conduct several simulations in corridor and bottleneck to verify and validate the model.

The results show that the proposed model can effectively eliminate the oscillating phenomenon in the narrow corridor persisting in the collision-free speed model. Moreover, it fits well with the experimental results in simulating the relationship between the density and speed of pedestrians in the corridor with periodic boundaries. It also performs well in the bottleneck scenario. On the one hand, it shows a visible enhancement in predicting the trajectories and velocities of the crowd and mitigates the backward movement of pedestrian effectively when compared with collision-free speed model. On the other hand, the model predicts the pedestrian flow with different bottleneck widths more accurately. In the future, further mechanisms of pedestrian's behavior, like the tendency to follow others and the polite behavior (e.g. way giving), can be introduced to the model.

CRediT authorship contribution statement

Sainan Zhang: Conceptualization, Methodology, Formal analysis, Investigation, Validation, Writing-Original Draft, Visualization. Jun Zhang: Conceptualization, Resources, Data Curation, Writing-Reviewing & Editing, Supervision, Funding acquisition. Mohcine Chraibi: Conceptualization, Software, Writing-Reviewing & Editing. Weiguo Song: Writing-Reviewing & Editing, Supervision.

Acknowledgement

The authors acknowledge the foundation support from the National Key Research and Development Program of China (Grant No. 2018YFC0808600), the National Natural Science Foundation of China (Grant No. U1933105, 71704168), the Anhui Provincial Natural Science Foundation (Grant No. 1808085MG217), the Fundamental Research Funds for the Central Universities (Grant No. WK2320000040, WK2320000043), the Visiting Professor International project at the University of Science and Technology of China (Grant No. 2019A VR35).

References

[1] Helbing D, Mukerji P. Crowd disasters as systemic failures: Analysis of the love parade disaster. EPJ Data Sci 2012. https://doi.org/10.1140/epjds7.

[2] Alaska YA, Aldawas AD, Aljerian NA, Memish ZA, Suner S. The impact of crowd control measures on the occurrence of stampedes during Mass Gatherings: The Hajj experience. Travel Med Infect Dis 2017. https://doi.org/10.1016/j.tmaid.2016.09.002.

[3] Chowdhury D, Santen L, Schadschneider A. Statistical physics of vehicular traffic and some related systems. Phys Rep 2000. https://doi.org/10.1016/S0370-1573(99)00117-9.

[4] Degond P, Appert-Rolland C, Moussaïd M, Pettré J, Theraulaz G. A Hierarchy of Heuristic-Based Models of Crowd Dynamics. J Stat Phys 2013. https://doi.org/10.1007/s10955-013-0805-x.

[5] Chraibi M, Seyfried A, Schadschneider A. Generalized centrifugal-force model for pedestrian dynamics. Phys Rev E - Stat Nonlinear, Soft Matter Phys 2010. https://doi.org/10.1103/PhysRevE.82.046111.

[6] Yang X, Wang Q. Crowd Hybrid Model for Pedestrian Dynamic Prediction in a Corridor. IEEE Access 2019. https://doi.org/10.1109/ACCESS.2019.2928556.

[7] Yang X, Yang X, Wang Q. Pedestrian evacuation under guides in a multiple-exit room via the fuzzy logic method. Commun Nonlinear Sci Numer Simul 2020. https://doi.org/10.1016/j.cnsns.2019.105138.

[8] Helbing D, Molnár P. Social force model for pedestrian dynamics. Phys Rev E 1995. https://doi.org/10.1103/PhysRevE.51.4282.

[9] Helbing D. Traffic and related self-driven many-particle systems. Rev Mod Phys 2001. https://doi.org/10.1103/RevModPhys.73.1067.

[10] Helbing D, Farkas I, Vicsek T. Simulating dynamical features of escape panic. Nature 2000. https://doi.org/10.1038/35035023.

[11] Chraibi M, Kemloh U, Schadschneider A, Seyfried A. Force-based models of pedestrian dynamics. Networks Heterog Media 2011. https://doi.org/10.3934/nhm.2011.6.425.

[12] Tordeux A, Chraibi M, Seyfried A. Collision-Free Speed Model for Pedestrian Dynamics. Traffic Granul. Flow ’15, 2016. https://doi.org/10.1007/978-3-319-33482-0_29.

[13] Fiorini P, Shiller Z. Motion planning in dynamic environments using velocity obstacles. Int J Rob Res 1998. https://doi.org/10.1177/027836499801700706.

[14] Dietrich F, Köster G. Gradient navigation model for pedestrian dynamics. Phys Rev E - Stat Nonlinear, Soft Matter Phys 2014. https://doi.org/10.1103/PhysRevE.89.062801.

[15] Ondřej J, Pettré J, Olivier AH, Donikian S. A synthetic-vision based steering approach for crowd simulation. ACM SIGGRAPH 2010 Pap. SIGGRAPH 2010, 2010. https://doi.org/10.1145/1778765.1778860.

[16] Van Berg J Den, Lin M, Manocha D. Reciprocal velocity obstacles for real-time multi-agent navigation. Proc. - IEEE Int. Conf. Robot. Autom., 2008. https://doi.org/10.1109/ROBOT.2008.4543489.

[17] Bovy, Stern. Route Choice: Wayfinding in Transport Networks. Springer Netherlands; 1990.

[18] Deroo C, Montuwy A, Degraeve B, Auberlet J-M, Olivier A-H, Granié M-A. Pedestrian collision avoidance on narrow sidewalk: a meeting between psychology and virtual reality 2019.

[19] Pelechano N, Brien KO, Silverman B, Badler N. Crowd simulation incorporating agent psychological models, roles and communication. First Int Work Crowd Simul 2005.

[20] Yao X, Lian Y, Wei C. A Markov Jump Approach to Modeling and Analysis of Pedestrian Dynamics. IEEE Access 2019. https://doi.org/10.1109/ACCESS.2019.2920992.

[21] Moussaïd M, Helbing D, Theraulaz G. How simple rules determine pedestrian behavior and crowd disasters. Proc Natl Acad Sci U S A 2011. https://doi.org/10.1073/pnas.1016507108.

[22] Lv W, Song WG, Ma J, Fang ZM. A two-dimensional optimal velocity model for unidirectional pedestrian flow based on pedestrian's visual hindrance field. IEEE Trans Intell Transp Syst 2013. https://doi.org/10.1109/TITS.2013.2266340.

[23] Batty M. Predicting where we walk. Nature 1997. https://doi.org/10.1038/40266.

519 [24] Turner A, Penn A. Encoding natural movement as an agent-based system: An
520 investigation into human pedestrian behaviour in the built environment. Environ
521 Plan B Plan Des 2002. https://doi.org/10.1068/b12850.

522 [25] Luo L, Fu Z, Cheng H, Yang L. Update schemes of multi-velocity floor field
523 cellular automaton for pedestrian dynamics. Phys A Stat Mech Its Appl 2018.
524 https://doi.org/10.1016/j.physa.2017.09.049.

525 [26] Wagoum AUK, Chraibi M, Zhang J, Lämmel G. JuPedSim: an open framework
526 for simulating and analyzing the dynamics of pedestrians. 3rd Conf. Transp. Res.
527 Gr. India, 2015.

528 [27] Xu Q, Chraibi M, Tordeux A, Zhang J. Generalized collision-free velocity model
529 for pedestrian dynamics. Phys A Stat Mech Its Appl 2019.
530 https://doi.org/10.1016/j.physa.2019.122521.

531 [28] Zhang J, Klingsch W, Schadschneider A, Seyfried A. Transitions in pedestrian
532 fundamental diagrams of straight corridors and T-junctions. J Stat Mech Theory
533 Exp 2011. https://doi.org/10.1088/1742-5468/2011/06/P06004.

534 [29] Liddle J, Seyfried A, Klingsch W, Rupprecht T, Schadschneider A, Winkens A.
535 An experimental study of pedestrian congestions: influence of bottleneck width
536 and length. ArXiv Prepr ArXiv09114350 2009.

537